most comprehensive list, which is, however, limited in extent, has been given by Ranganathan (1967), and are the results of an application of a procedure (Ranganathan, 1966) for determining the possible Σ values and corresponding angles of rotation associated with a particular axis of rotation. The authors have determined the axes of rotation and the corresponding angles of rotation (ω) for all twenty-four ways of describing each of the twenty-two coincidence-site relationships given in column 2 of Table 1. These results are presented in Table 2 with the limitation that only the form of the axes of rotation are given. However, an experimentally determined orientation relationship may be compared with the relationships presented in Table 2, thus allowing the operative coincidence-site relationship to be determined readily. The more convenient orientation relationship given in column 2 of Table 1 may then be adopted, and the further crystallographic information contained in Table 1 utilized directly.

In Table 2 the results are presented in multiples of three colums, the first, second and third column in every three gives the axis of rotation, the multiplicity and the angle of rotation (ω) respectively. For the [100], [110] and [111] symmetry axes the angles of rotation ($90-\omega$, $90+\omega$, $180-\omega$), ($180-\omega$) and ($120-\omega$, $120+\omega$) respectively also give rise to the coincidence-site relationships indicated in column 2. The relationship which gives the smallest value of ω for a particular value of Σ is indicated by an asterisk. Table 2 effectively gives the results of an application of the procedure described by Ranganathan (1966) for all possible rotations about axes with indices $[l_1\ l_2\ l_3]$ for $\{(l_1)^2+(l_2)^2+(l_3)^2\}<123$ which give rise to the coincidence site relationships with $\sum \leq 31$.

The authors are indebted to Mr E. B. Crellin for valuable discussions. The award of an S. R. C. studentship is acknowledged by one of us (AFA).

References

BEVIS, M. (1969). *Acta Cryst.* A**25**, 370.

BRANDON, D. G. (1966). *Acta Met.* **14**, 1479.

BRANDON, D. G., RALPH, B., RANGANATHAN, S. & WALD, M. (1964). *Acta Met.* **12**, 813.

FRIEDEL, G. (1926). *Leçons de Cristallographie,* Paris.

JASWON, M. A. (1956). *Mathematical Crystallography.* London: Longmans.

JASWON, M. A. & DOVE, D. B. (1955). *Acta Cryst.* **8**, 88.

LANGE, F. F. (1967). *Acta Met.* **15**, 311.

MORGAN, R. M. & RALPH, B. (1967). *Acta Met.* **15**, 341.

RANGANATHAN, S. (1966). *Acta Cryst.* **21**, 197.

RANGANATHAN, S. (1967). In *Field-Ion Microscopy,* Edited by J. HREN & S. RANGANATHAN. New York: Plenum Press.

SARGENT, C. M. (1968). *Trans. A.I.M.E.* **242**, 1188.

SCHOBER, T. & BALLUFFI, R. W. (1970). *Phil Mag.* In the press.

VAUGHAN, D. (1969). *Acta Cryst.* A**25**, S7.

Acta Cryst. (1971). A**27**, 179

The Effect of Refraction in the Small-Angle Diffraction of X-rays from Stacked Lamellae

BY J. M. SCHULTZ*

Department of Material Science, Stanford University, Stanford, California 94305, *U.S.A.*

(*Received* 25 *May* 1969 *and in revised form* 13 *April* 1970)

An expression for the scattering of X-rays from a regular stack of lamellae is developed, releasing the prior restraint that no refraction may occur. The effect of refraction is to cause deviations from the classical Bragg condition. Further, a condition of total reflection is shown to occur within systems whose lamellar spacings are greater than a critical value.

Statement of the problem

The analysis of X-ray scattering data generally proceeds through a consideration of the amplitude of scattering $A(\mathbf{S})$ as given by

$$A(\mathbf{S})=A_e(\mathbf{S})\int \varrho(\mathbf{X})\exp\{2\pi i\mathbf{S}\cdot\mathbf{X}\}dv_{\mathbf{x}}\,. \qquad (1)$$

Here, $A_e(\mathbf{S})$, ϱ, $\mathbf{X}$, $\mathbf{S}$, and $v_{\mathbf{x}}$ have their usual meanings: amplitude of scattering by an isolated electron, electron density, real space vector, reciprocal space vector, and real space volume. This expression is rigorously correct (in the kinematic approximation) only if (*a*) the medium is non-absorbing and (*b*) the vector $\mathbf{S}$ is permitted to vary as the X-ray beam traverses regions of differing refractive index. Indeed, absorptive and refractive corrections are not needed in the analysis of diffraction line breadths and peak positions; *e.g.*, the relative errors in atomic positional analysis are of the order of 10^{-5} and can safely be ignored. However, for the particular case of diffraction from a lamellar system whose elements are 100 Å or more in thickness both absorptive and refractive effects can become large. The under-

* On leave from Department of Chemical Engineering, University of Delaware, Newark, Delaware 19711, U.S.A.

lying reason for this increase in importance is the greater path length of the beam in passing through one lamella at a Bragg angle of some 10^{-2} rad. For instance, in a lamellar stack of alternating A and B sheets, each 100 Å thick, the Bragg angle for Cu $K\alpha$ radiation is $3{\cdot}85 \times 10^{-3}$ radians and the path length of a ray penetrating either layer at that angle is $2{\cdot}6\mu$! The absorption of the X-ray beam in passing through such layers at the Bragg angle is great enough to reduce the effective number of scattering plates to a relatively small number and to cause a broadening of the X-ray diffraction line. This effect has been treated in a previous paper (Schultz, 1970). In the present work, we shall treat the effect of the change of the scattering vector **S** as it passes through alternating lamellar regions of higher and lower refractive index.

The idealized situation is depicted in Fig. 1. We envision a regular, alternating stack of A and B lamellae, the stack itself embedded in a medium of the same average composition as the stack. The electron densities ϱ and the refractive deviants δ of the three regions considered are ϱ_{ave}, ϱ_1, ϱ_2 and δ_{ave}, δ_1, δ_2. The normal Bragg path is exemplified by the dashed line and is to be compared with the new path $VWXYZ$. What is particularly to be noted is that the ray passing through the stack has a more tortuous path than it would have were it not bent in crossing the several phase boundaries. Clearly, the diffracting condition is altered by this consideration. In particular, the longer path requires a higher glancing angle than the θ predicted by the classical Bragg condition, in order that the diffracted rays may still emerge in phase in the medium of average density. As lamellae become thicker, the glancing angle will decrease until it corresponds to the critical angle for complete reflection. Lamellar spacings larger than this will exhibit only total reflection; no Bragg scattering will be present.

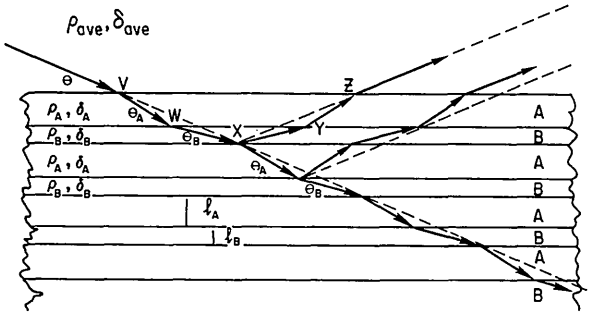

Fig. 1. Scattering from an alternating series of A and B platelets embedded in a medium whose properties are the mass averages of those of the A and B platelets.

In the following sections, these intuitive ideas are quantified. We shall see that deviations from the classical Bragg condition begin to become important somewhere in the range of 100 to 1000 Å in lamellar spacings, depending upon the scattering system. We shall see also that the condition of total reflection may be reached at an angle equivalent to that for diffraction. Lamellar spacings equal to or larger than that associated with the onset of total reflection show no diffraction effect.

Geometrical analysis of the refractive effect

The condition of constructive interference is defined by the geometry of Fig. 2. The system with which we work here is a regular, alternating stacking of A and B plates. The incident beam reaches the 'top' surface of the stack by passing through a medium whose properties are the average of the system. We shall take the mean density and refractive index in the stack to also be given by such averages. We let θ be the glancing angle for entrance to the stack and define θ_A and θ_B as in Fig. 2.

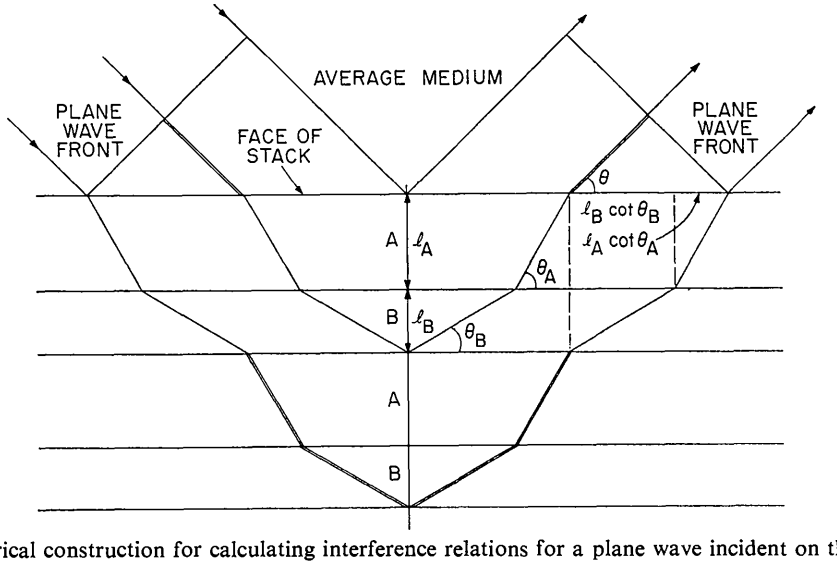

Fig. 2. Geometrical construction for calculating interference relations for a plane wave incident on the lamellar stack.

We shall represent the A and B lamellae by the vectors $\mathbf{l}_A$ and $\mathbf{l}_B$, such that l_A and l_B are the thicknesses of the plates and such that the directions of $\mathbf{l}_A$ and $\mathbf{l}_B$ are normal to the platelets. Finally, we take the wave vectors $|\mathbf{k}|=1/\lambda$ in the average medium, A lamellae, and B lamellae to be k_{ave}, k_A and k_B, respectively. Using these definitions, the condition for constructive interference becomes

$$\frac{p}{2}=\frac{k_A l_A}{\sin\theta_A}+\frac{k_B l_B}{\sin\theta_B} -(l_A\cot\theta_A+l_B\cot\theta_B)k_{ave}\cos\theta, \quad (2)$$

where p is an integer.

We now seek an equation written in terms of the average medium diffraction variables k_{ave} and θ. The condition (2) will then be directly comparable with the condition of in-phase scattering written according to a simple Bragg relation.

Recalling that the index of refraction for X-rays may be written as $n=1-\delta$, we can now write k_A and k_B in terms of k_{ave} and of the quantities δ_A, δ_B, and δ_{ave} in the three media and we can also write θ_A and θ_B in terms of θ, n_A, n_B, and n_{ave}. In all of the following we assume $\varrho_A>\varrho_B$. The wave vectors' magnitudes are thus

$$k_A=[1+(\delta_{ave}-\delta_A)]k_{ave} \quad (3)$$

$$k_B=[1-(\delta_B-\delta_A)]k_A\,. \quad (4)$$

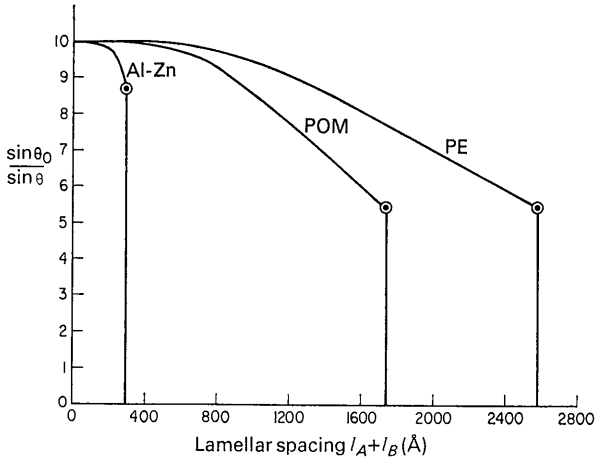

Fig. 3. Effect of material and period of stacking on the deviation of θ from the classical Bragg angle θ_0.

The angle θ_A is determined from the refractive condition

$$\cos\theta_A=[1-(\delta_{ave}-\delta_A)]\cos\theta\,. \quad (5)$$

Similarly,

$$\cos\theta_B=\frac{1}{[1-(\delta_B-\delta_A)]}\cos\theta_A\,. \quad (6)$$

We may now write the diffraction condition explicitly in terms of θ and the material constants δ_A and δ_B. We first note that the average value of δ is given by

$$\delta_{ave}=\frac{l_A}{l_A+l_B}\delta_A+\frac{l_B}{l_A+l_B}\delta_B=(1-X)\delta_A+X\delta_B\,. \quad (7)$$

For a polymeric system X can be considered the volume fraction crystallinity if the B lamella is a crystal and the A layer is amorphous. Using (7), the quanity $(\delta_A-\delta_{ave})$ found in (3) becomes

$$\delta_{ave}-\delta_A=X(\delta_B-\delta_A)=X\Delta\delta\,. \quad (8)$$

Using equations (3) to (8), the diffraction condition becomes

$$\begin{aligned}\frac{p}{2}&=\frac{k_{ave}l_A}{\sin\theta_A}[(1+X\Delta\delta)-\cos\theta_A\cos\theta]\\&+\frac{k_{ave}l_B}{\sin\theta_B}[(1-\Delta\delta)(1+X\Delta\delta)-\cos\theta_B\cos\theta]\\&=\frac{k_{ave}l_A}{\sin\theta}\left\{\frac{(1+X\Delta\delta)-(1-X\Delta\delta)\cos^2\theta)}{[1-(1-X\Delta\delta)^2\cos^2\theta]^{1/2}}\right\}\\&+\frac{k_{ave}l_B}{\sin\theta}\left\{\frac{(1-\Delta\delta)(1+X\Delta\delta)-\left(\frac{1-X\Delta\delta}{1-\Delta\delta}\right)\cos^2\theta}{\left[1-\left(\frac{1-X\Delta\delta}{1-\Delta\delta}\right)^2\cos^2\theta\right]^{1/2}}\right\}.\end{aligned} \quad (9)$$

In general, $\Delta\delta$ will be of the order of 10^{-6}. Further, θ is expected to be of the order of 10^{-2} or smaller for periodicities of 10^2 Å or greater and for X-ray wavelengths of the order of 1 Å. Thus (9) can be simplified by using the appropriate approximations dealing with small deviations from unity and by neglecting products of small numbers. Using these approximations and noting that $X=l_B/(l_A+l_B)=1-l_A/(l_A+l_B)$, we have

Table 1. *Material parameters*

Material	ϱ (g.cm^{-3}) Phase A	ϱ (g.cm^{-3}) Phase B	$\delta_\infty\times10^6$ Phase A	$\delta_\infty\times10^6$ Phase B	X	$\Delta\delta_\infty\times10^6$
Polyethylene	0·85[a]	1·00[a]	3·47	2·95	0·7[c]	0·52
Polyoxymethylene	1·25[a]	1·51[a]	4·93	3·94	0·7[c]	0·99
78 Al–22 Zn	2·70[b]	6·51[b]	15·49	9·68	0·25[d]	5·81

a Miller & Nielsen (1961).
b Barrett & Massalski (1966).
c Typical values.
d Hansen (1936).

$$\frac{p}{2k_{ave}(l_A+l_B)} = \sin\theta_0 \simeq \frac{(1-X)}{\sin\theta} \times \left\{ \frac{\sin^2\theta + X\Delta\delta(2-\sin^2\theta)}{[\sin^2\theta + X\Delta\delta(2-2\sin^2\theta) - (X\Delta\delta)^2(1-\sin^2\theta)^{1/2}} \right\}$$

$$+ \frac{X}{\sin\theta} \left\{ \frac{\sin^2\theta - (1-X)\Delta\delta(2-\sin^2\theta) - (\Delta\delta)^2(1-\sin^2\theta + X\sin^2\theta)}{[\sin^2\theta - (1-X)\Delta\delta(2-2\sin^2\theta) - (3-4X+X^2)(\Delta\delta)^2(1-\sin^2\theta)]^{1/2}} \right\}$$

$$\simeq \frac{(1-X)}{\sin\theta}[\sin^2\theta + 2X\Delta\delta]^{1/2} + \frac{X}{\sin\theta}[\sin^2\theta - 2(1-X)\Delta\delta]^{1/2}$$

$$= \sin\theta \left\{ (1-X)\left[1 + \frac{2X\Delta\delta}{\sin^2\theta}\right]^{1/2} + X\left[1 - \frac{2(1-X)\Delta\delta}{\sin^2\theta}\right]^{1/2} \right\}. \quad (10)$$

Here θ_0 is the classically calculated Bragg angle. Equation (10) is our final expression for the diffraction from a lamellar system.

Application of the basic diffraction formula

Equation (10) can be used directly to evaluate the effect of refraction on the scattering of X-rays by lamellar systems. One need only first obtain values of the constants δ. Having these, the quotient $\sin\theta_0/\sin\theta$ can be plotted against $\sin\theta$ or $\sin\theta_0$. However, in order to depict more positively the morphological conditions of the problem, we have plotted $\sin\theta_0/\sin\theta$ *versus* l_A+l_B, the periodicity of stacking, deriving the periodicity from the condition $l_A+l_B=\lambda/2\sin\theta_0$. Fig. 3 shows the results of this calculation for the three typical lamellar systems, polyethylene (PE) of 70 volume per cent crystallinity, polyoxymethylene (POM) of 70 volume per cent crystallinity, and the spinodal alloy system 78 Al–22 Zn, the material parameters of which are shown in Table 1. This spinodal alloy was chosen to represent non-polymeric materials since it has been studied (Rundman & Hilliard, 1967) using X-ray small-angle scattering.

There are several notable features in Fig. 2. First, we notice that below 200 Å there is very little refraction effect for any system analyzed here. For the polymeric systems, the repeat spacings associated with a 5% correction are 710 and 960 Å for POM and PE respectively. Most published data fall below these regions; hence, corrections will be necessary only in extreme cases. Secondly, we notice cut-off values of l_A+l_B above which no diffraction is to be observed. These critical values correspond to the condition

$$(1-X)\frac{2\Delta\delta}{\sin^2\theta_c} = 1 .$$

At this critical angle θ_c the radical on the rightmost term of (10) becomes imaginary. Physically, what happens is that the X-ray, having passed through the less dense layer *A*, is totally reflected from the more dense *B*. The X-ray beam will then pursue a zigzag course through the stack, reflecting alternately from the top and bottom boundaries of the *A* layer. This condition is depicted in Fig. 4. Thus for all lamellar spacings larger than $(l_A+l_B)_c$, the reflection will be total and the small-angle intensity *versus* receiving angle curve will appear as shown schematically in Fig. 5. The degree of approach of the actual curve to the step function increases as the quantity $\varepsilon=(\lambda/4\pi)\mu/\Delta\delta$ approaches zero (Compton & Allison, 1935) (μ being the linear absorption coefficient of the denser lamellae); the deviation from a step function is a result of absorption of the X-ray reflecting platelets. In the three typical materials used as examples above, ε is of the order of 10^{-2}. Finally, we note that the magnitude of the refractive effect prior to total reflection is dependent very much on the value of *X*. This can be seen in Fig. 2. In Fig. 2, the two polymers have δ's differing by nearly a factor of 2. Their limiting values of $\sin\theta_0/\sin\theta$ are, nevertheless, identical. Further, it is easily seen that $\sin\theta_0/\sin\theta$ becomes unity at $X=0$ and $X=1$. The condition of greatest refractive correction occurs at $X=\frac{1}{2}$.

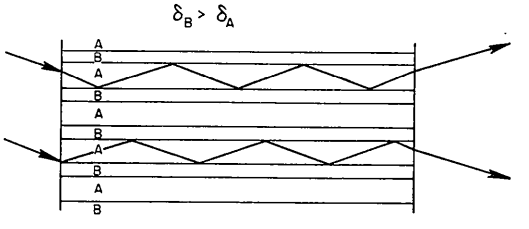

Fig. 4. The course of the 'channeled' X-ray beam in the condition of total reflection.

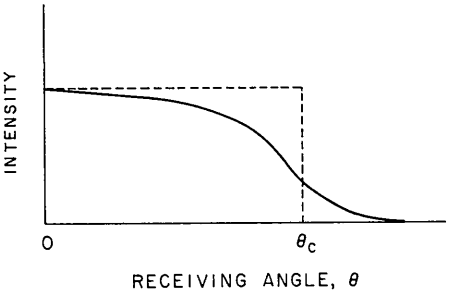

Fig. 5. Ideal intensity *versus* angle curve for the condition of total reflection (full curve). The broken curve represents step function approached asymptotically as $(\lambda/4\pi)\mu/\Delta\delta$ becomes very small.

Summary

It has been demonstrated that the increase in beam path due to changing refractive indices causes a substantial deviation from classical Bragg conditions at very small angles. The effect becomes more pronounced as the density difference between lamellar types increases and as the relative thickness of the two types approach each other. Below a critical angle θ_c diffraction is replaced by total reflection of the X-ray beam.

References

BARRETT, C. S. & MASSALSKI, T. B. (1966). *Structure of Metals*, Table A–6. New York: McGraw Hill.

COMPTON, A. H. & ALLISON, S. K. (1935). *X-rays in Theory and Experiment*. New York: Van Nostrand.

HANSEN, M. (1936). *Aufbau der Zweistofflegierungen*. Berlin: Springer.

MILLER, R. L. & NIELSEN, L. E. (1961). *J. Polymer Sci.* **55**, 643.

RUNDMAN, K. B. & HILLIARD, J. E. (1967). *Acta Met.* **15**, 1025.

SCHULTZ, J. M. (1970). *Acta Cryst.* A**26**, 93.

Acta Cryst. (1971). A**27**, 183

The Approximate Location of Centres of Molecules from Morphological Data

BY A. C. HAZELL

Department of Inorganic Chemistry, University of Århus, DK-8000 Århus C, Denmark

(*Received* 16 *July* 1970)

Hartman has shown how the centres of molecules may sometimes be located when the observed morphology is not that predicted by the Donnay–Harker law and how further information may be obtained by the periodic-bond-chain method. The method outlined here shows how the two methods may be combined, either by using structure-factor charts, or by a series summation analogous to a Fourier summation.

Introduction

Hartman (1968) has shown how it is possible to locate the centres of molecules for crystals which do not obey the Donnay & Harker (1937) law. He has also shown how additional information can be obtained about the centres by the periodic-bond-chain method.

The Donnay–Harker rule for crystal morphology leads to the expectation that the prominence of crystal forms should be in the order of the reticular densities (lattice points per unit area) of the corresponding planes. That is in the order of decreasing d_{hkl}, planes which correspond to space group absences being omitted from the list.

Hartman supposes that if a low order form $\{hkl\}$ is absent this is because the interplanar spacing is d_{hkl}/n where n is probably 2. If the centres of the molecules are at x_1, y_1, z_1, and x_2, y_2, z_2 then

$$(x_2-x_1)h+(y_2-y_1)k+(z_2-z_1)l=1/n\,. \qquad (1)$$

If x_1, y_1, z_1, and x_2, y_2, z_2 are related by symmetry it is possible to substitute the expressions for the equivalent positions and to solve equation (1).

One method of solving the equation is to regard the structure as being composed of point atoms at the centroids of the molecules and to use structure factor graphs for the planes corresponding to the absent forms to find the possible positions for the centroids.

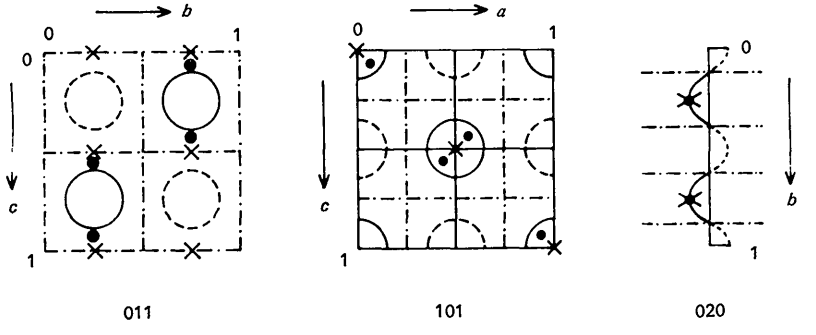

Fig. 1. α-$(NSOCl)_3$. Structure factor graphs for 011, 101, and 020. The nodes are shown by alternate dots and dashes. Positions of the centres of the molecules are shown by crosses, the experimental values thus ●.